Does roughness make elastic-adhesive contacts dissipative?

Giuseppe Carbone, Elena Pierro and Giuseppina Recchia

In this paper we investigate the adhesive contact between a rubber block and rigid randomly rough profiles, in loading and unloading conditions. The roughness is assumed to be described by a self-affine fractal on a limited range of wave-vectors. We employ a spectral method to generate such randomly rough surfaces with different root mean square roughness values and fractal dimensions. Calculations are performed for each profiles by means of an ad hoc numerical code previously developed by the authors.The calculated data are then statistically averaged, and the contact area, the applied load are shown as a function of the penetration, both for loading and un-loading conditions. It is found that the combination of adhesion forces and roughness leads to a hysteresis loading-unloading loop, which might be unexpected for perfectly elastic materials. This result is very interesting as it shows that energy can be lost simply as a consequence of roughness and van der Waals forces. Our calculations enable us to numerically quantify such an energy loss and, in particular, to assess the influence of the surface statistical properties and the energy of adhesion on the hysteresis process.

Keywords: *contact mechanics, roughness, adhesion, tribology*

1.Introduction

Contact mechanics between rough surfaces plays a crucial role in a large number of engineering applications, ranging from seals [1–4], boundary and mixed lubrication [5–8], adhesive systems, MEMS and NEMS and friction [9–12]. In this context, two main approaches have been developed to study the contact mechanics of an elastic body when it is brought into contact with a rough surface: (i) multiasperity contact theories [13–17] where the contact between the surfaces is modelled as an ensemble of randomly distributed Hertzian contacts between the asperities, and (ii) Persson's theory of contact mechanics [9, 18, 19], where the probability distribution of the contact pressure is shown to be governed by a diffusive process. Both approaches predict, with some differences, linearity between the contact area and the load in the limiting case of small loads. This has also been confirmed by some numerical and experimental studies [20–26], which have also shown that Persson's theory [9, 27] is able to capture, at least qualitatively, the physical mechanism behind contact mechanics of rough surfaces. On the other hand, other studies [17, 28] have shown that multiasperity contact theories predict linearity only for very small load values, whereas as the load is increased the theoretical predictions rapidly deviate from the asymptotic linearity. Moving from the pioneering investigation of Fuller and Tabor [29], there exists plenty of studies focusing on the adhesion of rough surfaces. These studies mainly use multiasperity models to describe the contact between rough surfaces. Unfortunately, multiasperity contact models only approximately describe the contact mechanics between rough surfaces, and as shown in [28], do not always give satisfactory results, as they neglect interaction and coalescence between asperities. However, multiasperity models have the merit of having clarified the main physical aspects of the contact problem. In this paper we utilize a completely different procedure which provides a fully numerically-exact solution of the equation governing the contact between rough surfaces. To deal with the adhesion contact problem we employ a methodology already presented by one of us in [35], based on a pure continuum mechanics approach and belonging to the class of Boundary Element Methods (BEMs) [10, 25]. The methodology, differently from finite element models (FEM) [22, 30], is much less expensive from a computational point of view and guarantee the achievement of converged results. FEM models have been also used to investigate the adhesion contact in presence of plastic deformation [30], neglected in our work because we focus on elastically soft materials, such as PDMS, which usually do not exhibit plastic deformation. Of course, real surfaces present 2D roughness, but there are mainly three reasons for studying 1D rough contacts: (i) first of all one should keep in mind that in order to obtain physically meaningful results, one needs to include in the analysis all the spectral components of the surface roughness (which can cover a range of scales of about 3-4 orders of magnitude), usually resulting in a strong increase of the computational cost. We observe that this problem is considerably reduced in case of 1D roughness; (ii) secondly we note that rough surfaces, encountered in many practical applications, are often strongly anisotropic mainly as a result of machining and surface treatments (e.g. unidirectional polished surface which presents wear tracks along the polishing direction, although the resulting roughness is not strictly 1D); (iii) thirdly it is possible to generate 1D rough surfaces which are equivalent, from the point of view of contact area vs. load relation, to 2D rough surfaces [32, 33]. Starting from the observation that many rough surfaces of practical interest are self-affine fractals (e.g. asphalt and concrete roads), the authors have recently presented a study [34] in which the role of the fractal dimension of the rough surface on the area-load and

penetration-load relations has been investigated, by analyzing the adhesion contact between a semi-infinite elastic space and periodic self-affine fractal 1D rough surfaces. Interestingly, both Persson's theory and multiasperity contact models show that, given the same material properties, the area vs. load relation is affected only by the moments of the PSD of the rough surface. However, the authors have shown [34] that the influence of fractal dimension D_f is negligible only in the range of linearity between the contact area and the applied load, whereas it becomes very significant at higher loads. Furthermore, the number of contacts is influenced by the applied load and by D_f , and the Dupre energy of adhesion strongly affect both the contact area and the PSD of the deformed profiles. In this paper we focus our attention on both the loading and the un-loading between a semi-infinite elastic space and periodic self-affine fractal 1D rough surfaces. We investigate, in particular, the influence of adhesion forces and surface roughness on the loading-unloading loop, and we show that energy can be lost simply as a consequence of roughness and van der Waals forces. We numerically quantify such an energy loss and the influence of the fractal dimension D_f and of the Dupre energy of adhesion on this hysteresis process is assessed.

2.The numerical model

In this Section we briefly summarize the numerical methodology presented in [10, 17, 20, 21]. We consider a periodic contact where an elastic layer of thickness d is interposed between a flat rigid plate (upper surface) and a periodically rough rigid substrate with wavelength λ (bottom surface) as shown in Fig. 1.

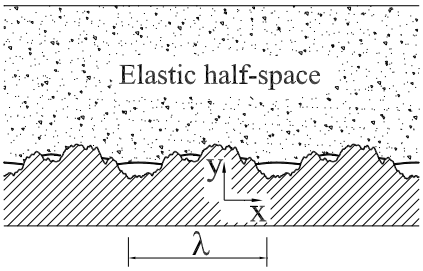

Fig. 1 An elastic half-space in contact with a periodic randomly rough rigid substrate of wavelength λ.

We consider the case of randomly rough surfaces with roughness in only one direction (i.e. 1D roughness). Of course real surfaces are 2D rough, but there are some good reasons for studying 1D rough contacts: (i) first of all one should keep in mind that in order to obtain physically meaningful results, one needs to include in the analysis all the spectral components of the 2D surface roughness (covering a range of scales of about 3-4 orders of magnitude). This results in a very strong increase of the computational cost, especially when the adhesive interaction is described in terms of surface energy, since the total energy of the system (which needs to be minimized to solve the contact problem) is a functional of the contact area contours. This problem is considerably reduced in case of 1D roughness, as, in this case, the total energy is a function of the coordinates of the endpoints of each contact segment; (ii) thirdly it is possible to generate 1D rough surfaces which are equivalent, from the point of view of contact area vs. load relation, to 2D rough surfaces [22, 23]. Therefore, we assume that the problem at hand is a periodic plane problem, i.e. the stress, displacement and strain fields depends only on the x and y coordinates and have a periodicity λ. Figure 2 shows the total displacement u_{tot} of the substrate, the average displacement u_m of the boundary of the deformed layer, and the penetration of the rigid substrate into the elastic layer.

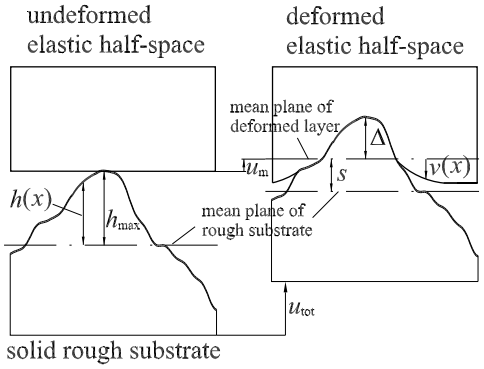

Fig. 2 A schematic representation of elastic displacement field at the interface, as they occur during approaching the substrate to the elastic solid by a quantity u_{tot}. Observe that u_{tot} is the sum of the mean displacement u_m of the elastic body and substrate penetration Δ. Also the interfacial displacement and the separation s between the two surfaces are shown.

These three quantities are shown to satisfy the following relation

$$u_{tot} = \Delta + u_m. \tag{1}$$

We will focus on the pressure distribution $\sigma(x)$ and interfacial displacement fluctuation $v(x) = u(x) - u_m$. In [10] and [35] it has been shown that the unknown pressure distribution in the contact area can be determined by solving the following Fredholm integral equation of the first kind with a logarithmic kernel

$$-\int_{\Omega} G(x-s)\sigma(s)ds = \left[h(x) - h_{\max}\right] + \Delta; \quad x \in \Omega \tag{2}$$

where $\Omega = \cup^{L}_{i=1} [a_i, b_i]$ is the unknown contact domain. The quantities a_i and b_i are the unknown coordinates of i-th contact patch with $a_i < b_i$ and i = 1, 2, ..., L, where L is the unknown number of contacts. In

Eq. (2), assuming the elastic layer is infinitely thick (i.e. $d \to +\infty$), the kernel is

$$G(x) = \frac{2(1-\upsilon^2)}{\pi E} \log\left[2\left|\sin\left(\frac{kx}{2}\right)\right|\right]. \quad (3)$$

and represents the Green function of the semi-infinite elastic body under a periodic loading, i.e. it represents the displacement $v(x)=u(x)-u_m$ caused by the application of a Dirac comb with peaks $\delta(x - n\lambda)$ separated by a distance λ. Here E and ν are Young's modulus and Poisson's ratio of the elastic layer. In Eq. (2) the quantity $h(x)$ represents the height of the rough profile from its mean plane. Since we are considering a periodic problem $h(x)$ can be represented in exponential form

$$h(x) = \sum_{m=-\infty}^{+\infty} a_m e^{imq_0 x}. \quad (4)$$

where the fundamental wavevector $q_0 = 2\pi/\lambda$, m the wavenumber, $a_m = |a_m|\, e^{i\phi m}$ and m-th the phase of the m-th spectral component, uniformly distributed in the interval [0, 2π [.

Also we have defined in Eq. (2) the quantity $h_{max}=max[h(x)]$, which is the maximum height of the substrate roughness. Once the pressure distribution is known the elastic displacements at the interface can be easily determined through the equations

$$\begin{aligned} v(x) &= -\int_\Omega G(x-s)\sigma(s)ds; x \in D-\Omega \\ v(x) &= h(x) - h_{\max} + \Delta; x \in \Omega. \end{aligned} \quad (5)$$

where D = [$-\lambda/2$, $\lambda/2$]. Of course for an infinitely thick layer ($d \to +\infty$ as in our case) the average displacement u_m is also infinitely large except when the ν = 0.5, but the difference $v(x) = u(x)-u_m$ is always finite [10, 5] and can be interpreted as the additional elastic displacement of the solid due to the presence of roughness at the interfaces. In order to close the system of equations we need an additional condition to determine the yet unknown contact domain Ω. To this end (see also Ref. [35]), we first observe that for any penetration Δ, we can calculate the pressure distribution at the interface through Eq. (2), and the interfacial elastic displacement through Eq. (5), as functions of the unknown coordinates a_i and b_i of the i-th contact area. To calculate the exact values of the quantities a_i and b_i at equilibrium, given isothermal conditions, we need to minimize the interfacial free energy $U_{tot}(a_1, b_1, ..., a_L, b_L, \Delta)$ of the system at fixed penetration Δ. The free interfacial energy (see [35]) is

$$U_{tot} = U_{el} + U_{ad} \quad (6)$$

where the interfacial elastic energy U_{el} is [25]

$$\begin{aligned} &U_{el}(a_i, b_i, ..., a_L, b_L, \Delta) = \\ &\frac{1}{2}\sum_{i=1}^{L}\int_{a_i}^{b_i}[\sigma(x)[h(x) - h_{\max} + \Delta]dx. \end{aligned} \quad (7)$$

The adhesion energy is

$$\begin{aligned} &U_{ad}(a_i, b_i, ..., a_L, b_L) = \\ &-\gamma\sum_{i=1}^{L}\int_{a_i}^{b_i}\sqrt{1+[h'(x)]^2}\,dx \end{aligned} \quad (8)$$

where γ is the work of adhesion. Eqs. (2), (5), together with the requirement that the interfacial free energy U_{tot} is a (local) minimum at equilibrium, constitute a set of closed equations which allows, for any given penetration Δ, to determine the coordinates a_i and b_i of each contact spot, the pressure distribution at the interface, and all other thermodynamic quantities. For the numerical implementation the reader is referred to [25, 35]. The numerical simulations have been carried out for a randomly rough profile with PSD

$$\begin{aligned} C_R(q) &= C\left(\frac{|q|}{q_{\min}}\right)^{-(2H+1)}; q \in [q_{\min}, q_{\max}] \\ C_R(q) &= 0; q \notin [q_{\min}, q_{\max}] \end{aligned} \quad (9)$$

where H is the Hurst exponent of the randomly rough profile. It is related to the fractal dimension $D_f = 2 - H$. In Eq. (9) $q_{min} = n_0 q_0$ and $q_{max} = N q_{min}$.

2.2 Results

We assume that the elastic block is a soft perfectly elastic material with elastic modulus E = 1 MPa and Poisson's ratio ν = 0.5. For each rough profile results have been averaged over 10 different realizations. The profiles have root mean square roughness $h_{rms} = \langle h^2 \rangle^{1/2} =$ 1 μm. The spectral components of our profiles are given by Eq. (9) and cover the wave-vector range from $q_{min} = n_0 q_0$ up to $q_{max} = N q_{min}$, outside this range the PSD is zero. We have considered $\lambda = 2\pi/q_0 = 6.28$ mm, $q_{min} = 10 q_0$, and $q_{max} = 100 q_{min}$. We note that once h_{rms}, q_{min}, and q_{max} are fixed, changing the Hurst exponent (i.e., the fractal dimension of the surface) also determines a modification of the average square slope $m_2 = \langle h'^2 \rangle = \int q^2 C_R(q) dq$ of the surface. For each generated rough profile [36] the numerical calculations have been carried out for different values of the separation $s = h_{max} - \Delta$. In Fig. 3 we show three different shapes of the deformed profile at three different values of the separation: s = 92 μm, s = 51 μm, and s = 20 μm, for (a) loading and (b) unloading conditions. The work of adhesion is $\gamma = 0.01$ J/m^2. The rigid rough substrate profile has a fractal dimension $D_f = 1.2$. In Fig. 3 the value s = 20 μm is the minimum value of separation at which the unloading process begins to take place after loading. Therefore at s = 20 μm the shape of the deformed profile is the same not depending on what condition (i.e., loading or unloading) is being considered. However, as the unloading proceeds further and the elastic block is moved away from the contact, the shape of the deformed profile significantly changes compared to the loading case (see s = 51, and 92 μm).

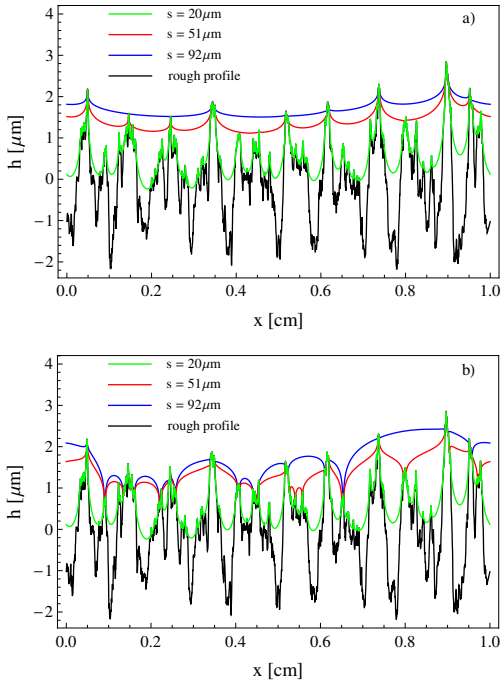

Fig. 3 The deformed shapes of the elastic body at three different separations, s = 92 μm, s = 51 μm, and s = 20 μm, and the rough rigid substrate profile, for (a) loading and (b) unloading. The work of adhesion is $\gamma = 0.01$ J/m^2, and the rigid rough substrate profile has a fractal dimension $D_f = 1.2$.

During unloading, unstable local pull-off events occur at random locations leading to pronounced differences between the loading and unloading processes. Such different behaviors can be indirectly observed in in Fig. 4, where the PSD of the rigid substrate profile (fractal dimension $D_f = 1.2$, non-dimensional penetration $\tilde{\Delta}=\Delta/h_{max}= 0.4$) has been compared to the PSD of the deformed shape of the elastic body during loading and unloading conditions, for $\gamma = 0.01$ J/m^2[Fig. 4(a)] and $\gamma = 0.04$ J/m^2 [Fig. 4(b)]. At first we remark that for large wave vectors q, the PSDs of the deformed profile, either in loading or unloading conditions (blue and red curves respectively), run parallel to the PSD of the rigid rough profile. This is due to the fact that, for $0.5 <H< 1$, full contact always occurs between the elastic block and the short wavelength corrugation of the rough rigid profile, (see Fig. 3). In fact, we can easily estimate the threshold wavelength l_{th} below which full contact occurs between solid and the rigid rough substrate. To this end consider that for a fractal surface the amplitude $A(q) = 2|a(q)|$ of each single wavy corrugation scales as $A(q)/A(q_{min}) \sim (q_{min}/q)^H$ where $A(q_{min})$ is of order of the rms roughness h_{rms} of the substrate. Now assume that the elastic slab makes contact with the surface on a region of size $l = 2\pi/q$ in this case, assuming $A(q) << l$, the change of elastic energy stored in the body can be shown to be $\Delta U_{el}=El^2A(q)$ whereas the change of adhesion energy upon contact is $\Delta U_{ad}\sim-\gamma l^2$. Therefore full contact will occur when the change of total energy $\Delta U_{tot} = \Delta U_{el} + \Delta U_{ad}$ upon contact is $\Delta U_{tot}< 0$. In this case the contact will occur on a single connected region, otherwise it will be split in many different contact spots. The condition $\Delta U_{tot}< 0$ gives $EA(q) < \gamma$, i.e., $A(q) < \delta = \gamma/E$ where δ is called the adhesion length. Using $A(q)/A(q_{min})\sim(q_{min}/q)^H$ one gets $l< 2\pi/q_{min})[\delta/A(q_{min})]^{1/H} = l_{th}$. In our case we get $l_{th} \approx$ 2–12 μm depending on the value of the energy of adhesion. Therefore, during loading, at scales below this threshold value l_{th} we will observe the formation of small contacts where the elastic solid conforms to the rigid substrate, thus leading to the observed trend of PSD (see Fig. 4), which, indeed, runs parallel to the PSD of the rigid rough profile.

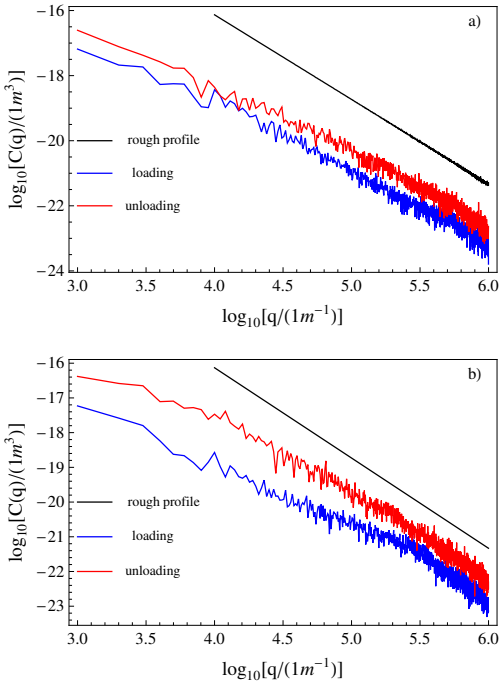

Fig. 4 The PSD of the rigid substrate profile with fractal dimension $D_f = 1.2$, compared to the PSD of the deformed shape of the elastic body at fixed non dimensional penetration $\tilde{\Delta}= \Delta/h_{max} = 0.4$, obtained for (a) $\gamma = 0.01$ J/m^2 and (b) $\gamma = 0.04$ J/m^2, for loading (blue curves) and unloading (red curves) conditions.

At smaller spatial frequencies the contact is, instead, split in many different disconnected regions [36]. When the PSDs of the deformed profile are compared at different values of the penetration (see Fig. 5), an interesting different behavior between loading and unloading can be observed. In particular, we note that, during loading, the PSD of the deformed surface is very sensitive to the penetration value $\tilde{\Delta}$ [Fig. 5(a)], while this sensitivity is much less pronounced during unloading [Fig. 5(b)], at least for relatively large values

of the energy of adhesion $\gamma = 0.04$ J/m^2 . In Fig. 6 the normalized real contact area A/A0 is shown, for different values of average square slope of the profile $m_2=\langle h'^2\rangle$ and adhesion energy γ , as a function of the dimensionless quantity $\tilde{\sigma}/\sqrt{m_2}$, where $\tilde{\sigma}=2\sigma/(E^*q_0h_{max})$. However, in our case, this linearity is not observed, especially when the two surfaces are moved apart (unloading). More importantly, given the same applied load, the contact area during unloading is much larger than during loading, thus leading to strong hysteresis. This is even more clear in Fig. 7(a) where the dimensionless load $\tilde{\sigma}$ is plotted vs. the non-dimensional penetration $\tilde{\Delta}$.

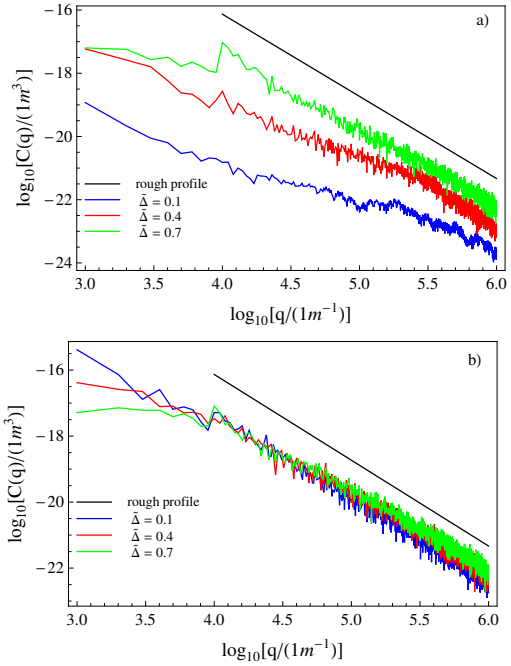

Fig. 5 The PSD of the rigid substrate profile with fractal dimension $D_f = 1.2$, compared to the PSD of the deformed shape of the elastic body, obtained for $\gamma = 0.04$ J/m^2, (a) for loading and (b) unloading conditions, for different values of the non-dimensional penetration $\tilde{\Delta}= \Delta/h_{max}$.

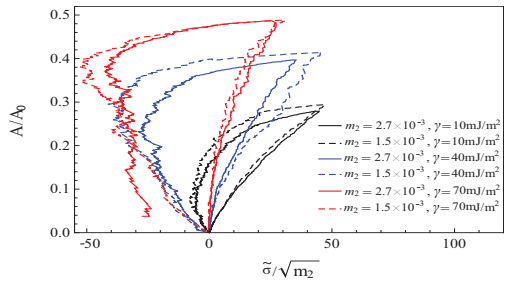

Fig. 6 The true contact area *A/A*0 as a function of the dimensionless quantity $\tilde{\sigma}/m_2^{1/2}$ for two different Hurst exponents $H = 0.8$ ($m_2= 2.7 \times 10^{-3}$), $H = 0.9$ ($m_2=1.5\times 10^{-3}$), and for three different values of energy of adhesion, $\gamma = 0.01$ J/m^2 (black curves), $\gamma = 0.04$ J/m^2 (blue curves), and $\gamma = 0.07$ J/m^2 (red curves). As predicted by the theories, there is a marginal influence of the fractal dimension on the true contact area at small loads under loading conditions. The influence of *Df* becomes important during unloading. This leads to the formation of a hysteresis loading-unloading loop, which is strongly affected by the adhesion energy γ.

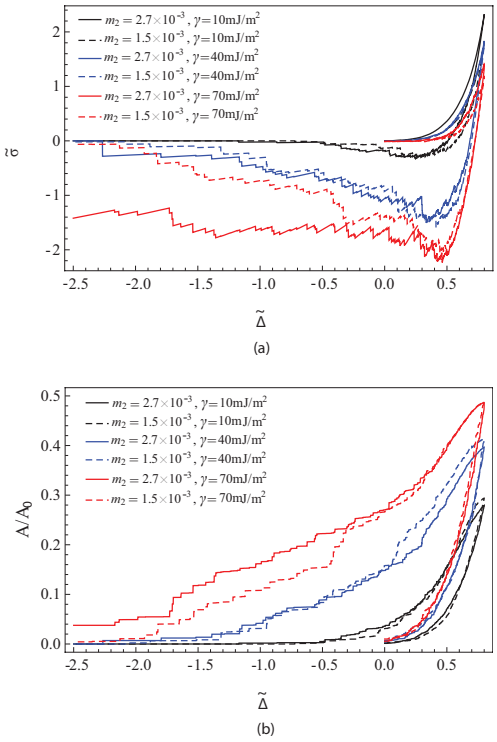

Fig. 7 The dimensionless load $\tilde{\sigma} = 2\sigma/(E^*q_0h_{max})$ (a) and the quantity *A/A*0 (b) as a function of the non-dimensional penetration $\tilde{\Delta}$, for two different Hurst exponents $H = 0.8$ ($m_2= 2.7 \times 10^{-3}$), $H = 0.9$ ($m2 = 1.5 \times 10^{-3}$), and for three different values of energy of adhesion, γ=0.01 J/m^2 (black curves), $\gamma = 0.04$ J/m^2 (blue curves), and γ= 0.07 J/m^2 (red curves).

It is noteworthy to observe that increasing the energy of adhesion γ leads to a strong increase of hysteresis loop [see Fig. 7(a)]. The origin of this behavior is twofold, as increasing γ necessarily leads to: (i) an increase of number of contact patches, and (ii) to an increase of the size of each single contact patch. This, in turn, determines an enhancement of SSH (Small-Scale-Hysteresis) and LSH (Large-Scale-Hysteresis) phenomena [36], i.e., to a large increment of energy dissipation during the loading-unloading loop. Figure 7(b) shows the reduced real contact area A/A0 as a function of the dimensionless penetration $\tilde{\Delta}$ for two different Hurst exponents H = 0.8 ($m_2 = 2.7 \times 10^{-3}$), H = 0.9 ($m_2 = 1.5 \times 10^{-3}$), and for three different values of

energy of adhesion, $\gamma = 0.01$ J/m^2 (black curves), $\gamma = 0.04$ J/m^2 (blue curves), and $\gamma = 0.07$ J/m^2 (red curves). An estimation of the dimensionless energy loss during the entire loading-unloading cycle, for different values of the average square slope of the profile, is given in Table I.

Table 1 The dimensionless energy loss.

	γ=0.01 J/m^2	γ=0.04J/m^2	γ=0.07J/m^2
m_2=5.1x10^{-3}	-	26.6	42.83
2.7x10^{-3}	3.44	19.36	49.25
1.5x10^{-3}	2.59	17.91	28.15

2.3 Conclusions

In this work we have studied the adhesive contact between a rubber block and rigid randomly rough profiles, in loading and unloading conditions. The roughness has been assumed to be described by a self-affine fractal on a limited range of wave-vectors. A spectral method to generate such randomly rough surfaces with different root mean square roughness values and fractal dimensions has been employed. Calculations have been performed for each profile by means of an ad hoc numerical code previously developed by the authors. The calculated data have been then statistically averaged, and the influence of the fractal dimension D_f on the contact area has been investigated. We have found that at small load (i.e., in the linear regime between contact area and load) the influence of D_f is negligible in the loading condition, while in the unloading condition the influence of D_f becomes important. Moreover, the contact area and the applied load have been shown as a function of the penetration, both for loading and un-loading conditions. Interestingly we have observed that the combination of adhesion forces and roughness leads to a hysteresis loading-unloading loop, which might be unexpected for perfectly elastic materials. This means that energy can be lost as a consequence of roughness and van der Waals forces, and we have numerically quantified such an energy loss. Our results have shown that the fractal dimension D_f and the Dupre energy of adhesion strongly influence this hysteresis process. Moreover, because of its relevance in the field of mixed lubrication and seals, we have calculated the probability density function (PDF) of the local separations between the deformed profile and rough rigid surface, in loading and unloading conditions. We have found that the PDF of the local separations differ in the two cases, and this is because of the different shape of the deformed profiles, related to the work of adhesion.

References

[1] B.N.J. Persson and C. Yang. J. Phys. Condens. Matter 20, 315011, 2008.
[2] B. Lorenz and B.N.J. Persson. Eur. Phys. J. E 31, 159-167, 2010.
[3] F. Bottiglione, G. Carbone, L. Mangialardi and G. Mantriota. J. Appl. Phys. 106, 104902, 2009.
[4] F. Bottiglione, G. Carbone and G. Mantriota. Tribol. Int. 42, 731–737, 2009.
[5] M. Scaraggi, G. Carbone, B.N.J. Persson and D. Dini. Soft Matter, submitted, 2011.
[6] M. Scaraggi, G. Carbone, B.N.J. Persson and D. Dini. Soft Matter, submitted, 2011.
[7] M. Scaraggi and G. Carbone. J. Mech. Phys. Solids 58, 1361-1373, 2010.
[8] M. Scaraggi, G. Carbone, and D. Dini. Tribol. Lett4(2), 169-174, 2011.
[9] B.N.J. Persson. J. Chem. Phys. 115, 3840, 2001.
[10] G. Carbone and L. Mangialardi. J. Mech. Phys. Solids 52, 1267-1287, 2004.
[11] Y.P. Zhao, L. S. Wang and T. X. Yu. J. Adhes. Sci. Technol. 17, 519-546, 2003.
[12] G. Carbone, B. Lorenz, B.N.J. Persson and A. Wohlers. European Phys. J. E 29, 275–284,2009.
[13] J.A. Greenwood and J.B.P. Williamson. Proc. R. Soc. London A 295, 300, 1966.
[14] A.W. Bush, R.D. Gibson and T. R. Thomas. Wear 35, 87, 1975.
[15] T. R. Thomas. Rough Surfaces, Longman Group Limited, New York, 1982.
[16] J.A. Greenwood. Wear 261 191-200, 2006.
[17] G. Carbone. J. Mech. Phys. Solids 57, 1093–1102, 2009.
[18] B.N.J. Persson. Eur. Phys. J. E 8, 385, 2002.
[19] B.N.J. Persson. Surface Sci. Reports 61, 201–227, 2006.
[20] C. Yang, U. Tartaglino and B. N.J. Persson. European Phys. J. E 19, 47-58, 2006.
[21] M. Borri-Brunetto, B. Chiaia and M. Ciavarella. Comput. Methods Appl. Mech. Eng. 190,6053, 2001.
[22] S. Hyun, L. Pei, J.-F Molinari and M. O. Robbins. Phys. Rev. E 70, 026117, 2004.
[23] C. Campañà and M. H. Müser. Phys. Rev. B 74, 075420, 2006.
[24] C. Campañà. Phys. Rev. E 78, 026110, 2008.
[25] G. Carbone, M. Scaraggi and U. Tartaglino. European Phys. J. E 30, 65–74, 2009.
[26] M. Benz, K. J. Rosenberg, E. J. Krame and J. N. Israelachvili. J. Phys. Chem. B 110, 11884–11893, 2006.
[27] B.N.J. Persson. J. Phys.: Condens. Matter 20, 312001, 2008.
[28] G. Carbone, F. Bottiglione. J. Mech. Phys. Solids 56, 2555-2572, 2008.
[29] K.N.G. Fuller and D. Tabor, Proc. R. Soc. A-Math. Phys. Eng. Sci., 345, 327-342, 1975.
[30] Pei L. , Hyun S., Molinari J.F., Robbins M.O. J. Mech. Phys. Solids 53, 2385, 2005.
[31] L. X. Zhang and Y. P. Zhao. J. Adhes. Sci. Technol. 18, 715-729, 2004.
[32] G. Carbone, B. Lorenz, B.N.J. Persson and A. Wohlers. European Phys. J. E 29, 275–284, 2009.
[33] G. Carbone, M. Scaraggi and C. Putignano. in preparation.
[34] G. Carbone, E. Pierro, Journal of Adhesion Science and Technology 26, 2555-2570, 2012.
[35] G. Carbone and L. Mangialardi. J. Mech. Phys. Solids 56, 684-706, 2008.
[36] G. Carbone, E. Pierro, G. Recchia, Physical Review E - Statistical, Nonlinear, and Soft Matter Physics, Volume 92, Issue 6, 2015.